© 2014. Published by The Company of Biologists Ltd | Journal of Cell Science (2014) 127, 4443–4456 doi:10.1242/jcs.152975

RESEARCH ARTICLE

Quantifying mRNA targeting to P-bodies in living human cells reveals their dual role in mRNA decay and storage

Adva Aizer*, Alon Kalo*, Pinhas Kafri, Amit Shraga, Rakefet Ben-Yishay, Avi Jacob, Noa Kinor and Yaron Shav-Tal‡

ABSTRACT

The 5′-to-3′ mRNA degradation machinery localizes to cytoplasmic processing bodies (P-bodies), which are non-membranous structures found in all eukaryotes. Although P-body function has been intensively studied in yeast, less is known about their role in mammalian cells, such as whether P-body enzymes are actively engaged in mRNA degradation or whether P-bodies serve as mRNA storage depots, particularly during cellular stress. We examined the fate of mammalian mRNAs in P-bodies during translational stress, and show that mRNAs accumulate within P-bodies during amino acid starvation. The 5′ and 3′ ends of the transcripts residing in P-bodies could be identified, but poly(A) tails were not detected. Using the MS2 mRNA-tagging system for mRNA visualization in living cells, we found that a stationary mRNA population formed in P-bodies during translational stress, which cleared gradually after the stress was relieved. Dcp2-knockdown experiments showed that there is constant degradation of part of the P-body-associated mRNA population. This analysis demonstrates the dual role of P-bodies as decay sites and storage areas under regular and stress conditions.

KEY WORDS: P-body, RNA dynamics, RNA quantification

INTRODUCTION

Processing bodies (P-bodies) are cytoplasmic foci found in all eukaryotic cells (Eulalio et al., 2007a; Kedersha and Anderson, 2009; Kulkarni et al., 2010; Decker and Parker, 2012). Many protein factors localize to P-bodies, including components of the 5′-to-3′ general degradation machinery, mRNA surveillance pathways and microRNA (miRNA)-associated gene silencing factors. Deadenylation-dependent mRNA decay is the major pathway in mammalian cells. It begins with the shortening of the 3′ poly(A) tail by the Pan2–Pan3 and Ccr4–Not1 complexes and poly(A)-specific ribonuclease (PARN) followed by 3′-to-5′ or 5′-to-3′ decay. The exosome is responsible for 3′-to-5′ degradation, whereas 5′-to-3′ degradation involves other factors, including the Dcp2 decapping enzyme, which is part of the decapping complex. This complex contains proteins, such as Dhh1 and Edc3, that enhance decapping and specifically interact with Dcp1, another major P-body component. The protein Hedls is required for bridging the interaction between Dcp1 and Dcp2 in higher eukaryotes and might promote the formation of the decapping complex (Fenger-Grøn et al., 2005; Bail and Kiledjian, 2006; Simon et al., 2006). The decapping complex is recruited by Lsm1–Lsm7, and then the removal of the cap structure occurs, which irreversibly marks the mRNA for degradation. The mRNA transcript is then susceptible to digestion by the Xrn1 exonuclease, yet another P-body resident (Parker and Song, 2004).

Electron microscopy studies of P-body structure in HeLa cells have shown 5–10 non-membranous cytoplasmic foci ranging from 150 to 350 nm in size (Yang et al., 2004; Cougot et al., 2012), which appear to comprise clusters of electron-dense strands of 8–10 nm in diameter (Yang et al., 2004). Various studies have shown that the number and size of P-bodies can vary depending on the organism, tissue, cellular phase or stress conditions. P-bodies have been identified in lower and higher eukaryotes (Ingelfinger et al., 2002; van Dijk et al., 2002; Sheth and Parker, 2003; Cougot et al., 2004) and observations in yeast and mammalian cells have shown that P-body numbers depend on cellular conditions, such as osmotic stress, UV light or glucose deprivation. For instance, in the latter case, both yeast and mammalian P-bodies increase in size and number (Teixeira et al., 2005; Takahashi et al., 2011; Iwaki and Izawa, 2012). P-body numbers and size also change as a result of the levels of free cytoplasmic mRNA (Teixeira et al., 2005; Aizer et al., 2008). Many of the above conditions also affect the translational status of the cell. Moreover in yeast, mRNAs undergoing translation are excluded from P-bodies, whereas non-translating mRNAs can assemble into P-bodies. This has led to the suggestion that P-body numbers are directly influenced by translation rates (Teixeira et al., 2005).

Although much has been revealed about the protein composition of P-bodies, less is known regarding the localization and fate of mRNAs inside mammalian P-bodies (Lykke-Andersen, 2002; Bhattacharyya et al., 2006; Cougot et al., 2012). It has been demonstrated that non-degradable mRNAs accumulate in yeast P-bodies, and massively amassed in strains with downregulated Xrn1 or decapping activity, thus initially implicating these structures as participating in mRNA decay (Sheth and Parker, 2003). Decapping has been suggested to take place inside P-bodies because the decapping proteins are enriched within P-bodies, but direct evidence of decay in mammalian P-bodies is lacking (Izaurralde, 2009). By contrast, there is evidence from yeast that P-bodies are not only sites of mRNA decay, but can also be involved in the storage of translationally silent mRNAs that are capable of re-entering the translation machinery in response to altered cellular conditions (Brengues et al., 2005; Teixeira et al., 2005; Bhattacharyya et al., 2006; Parker and Sheth, 2007; Lavut and Raveh, 2012). Additionally, it has been found that P-body structures disassemble

The Mina & Everard Goodman Faculty of Life Sciences and Institute of Nanotechnology, Bar-Ilan University, Ramat Gan 52900, Israel.
*These authors contributed equally to this work

‡Author for correspondence (Yaron.Shav-Tal@biu.ac.il)

Received 10 March 2014; Accepted 5 August 2014

Journal of Cell Science

Journal of Cell Science (2014) 127, 4443–4456 doi:10.1242/jcs.152975

when RNA interference (RNAi) activity was downregulated in mammalian cells by blocking small interfering RNA (siRNA) or miRNA biogenesis pathways. However, mRNA decay activities continued in the cells even when no P-body structures were observed (Pauley et al., 2006; Eulalio et al., 2007b).

The aim of this study was to examine the dynamics of specific mRNAs inside mammalian P-bodies. Under normal cellular conditions, mRNA is not readily detectable in P-bodies. We found that amino acid starvation, which leads to translational stress (Harding et al., 2000; Kimball, 2002), induces mRNA accumulation in P-bodies. We thus could study the fate of mRNAs localizing to P-bodies during translational stress and following release from stress. In order to examine mRNA dynamics within P-bodies in living cells, we used the MS2 system that allows visualization of mRNA transcripts. Using three different gene expression systems (Ben-Ari et al., 2010; Mor et al., 2010; Brody et al., 2011) we followed, for the first time, the internal dynamics of mRNA localization in P-bodies, and are able to present a dynamic picture of transcript accumulation in P-bodies under translational stress conditions, showing that P-bodies act as both mRNA decay sites and storage sites.

RESULTS

Amino acid starvation leads to mRNA-dependent P-body assembly

In order to study the fate of mammalian mRNAs in P-bodies, we searched for a treatment that would enhance mRNA accumulation in P-bodies. In yeast, it has been demonstrated that various nutritional stresses lead to mRNA targeting to P-bodies, such as glucose depletion (Teixeira et al., 2005; Takahashi et al., 2011), osmotic stress, UV light (Teixeira et al., 2005) and acidic stress (Iwaki and Izawa, 2012). mRNA has been shown to enter P-bodies during translational shutoff, for either decay or for storage (Sheth and Parker, 2003; Brengues et al., 2005). We found that applying amino acid translational stress to mammalian cells by amino acid starvation induced the formation of P-bodies, as well as mRNA localization within them. The following experiments describe the characterization of the experimental system.

Amino acid starvation was achieved by use of EBSS medium lacking amino acids but containing glucose. After incubation of human osteosarcoma U2OS cells in EBSS medium, P-body numbers significantly increased. Endogenous P-bodies were labeled with the Hedls P-body marker and numbers were found to be elevated from an average of 5±3 P-bodies/cell to 9±6 P-bodies/cells after 1 h in EBSS, and to 14±5 P-bodies/cell after 6 h (mean±s.d.) (Fig. 1A,B). Similar results were obtained in human colon carcinoma RKO cells and mouse embryonic fibroblasts (MEFs) (Fig. 1B). The enhancement in P-body numbers was not due to changes in the expression levels of Dcp1a and Dcp2 P-bodies protein as seen by western blotting (Fig. 1C; supplementary material Fig. S1A), indicating that increased P-body assembly was occurring from the free cytoplasmic pool of P-body proteins. Likewise, the negative effect of amino acid starvation on translation was observed with a doxycycline-induced protein in a Tet-On expression system (Brody et al., 2011) that will be further used for quantifying mRNA in P-bodies. The induced protein consists of a β-globin-coding region fused to a CFP protein with a peroxisomal targeting

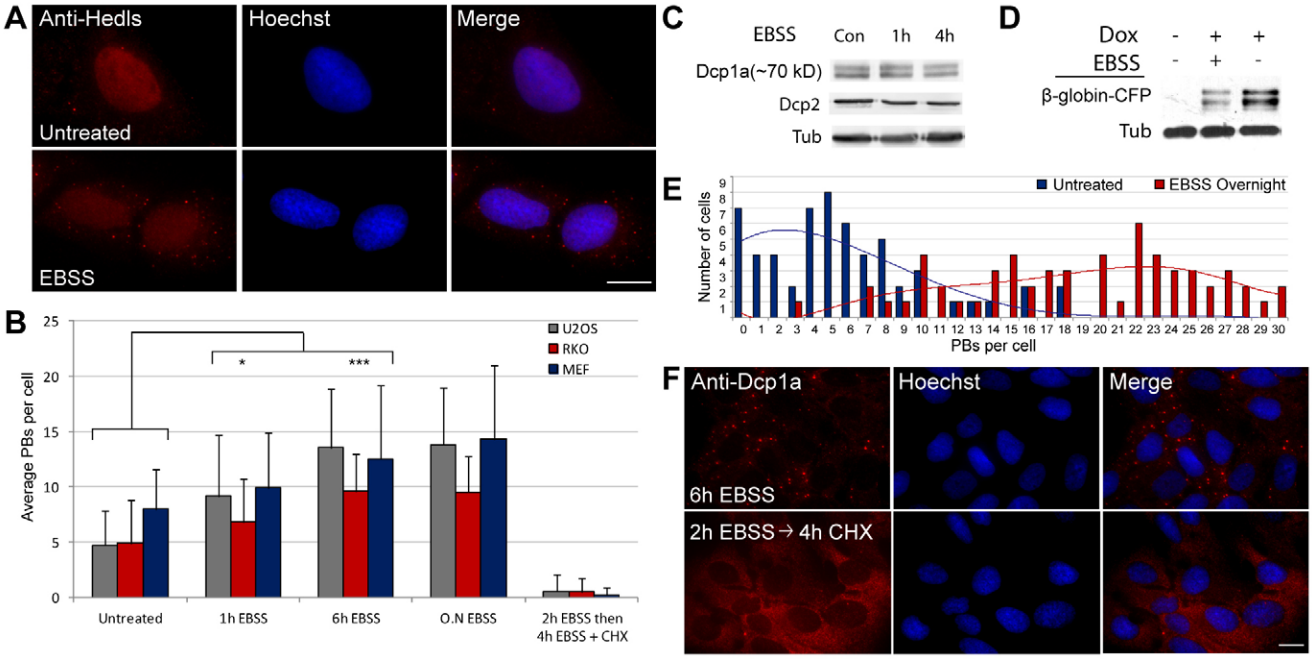

Fig. 1. Quantification and distribution of endogenous P-bodies during amino acid starvation. (A) Distribution of P-bodies (PBs) in U2OS cells during amino acid starvation (EBSS). Endogenous P-bodies were marked by anti-Hedls antibody (red); Hoechst DNA counter stain marks the nucleus (blue). (B) Count of endogenous P-bodies in U2OS, RKO and MEF cells during EBSS treatment (n=50 cells per time point, mean±s.d.). The right-most columns show counts of endogenous P-bodies in EBSS-treated cells in the presence of cycloheximide (CHX) (n=50 cells; mean±s.d.)*P<0.05, **P<0.01, ***P<0.005. (C) Immunoblot of the endogenous P-body markers, Dcp1a and Dcp2, during EBSS treatment for the indicated time. Con, control. (D) Cells containing a transcriptionally inducible gene (β-globin–CFP) were induced with doxycycline (Dox) with or without amino acids, and induced protein levels were observed by western blotting. (E) Distribution of P-body numbers per cell in untreated cells and after 24 h of EBSS starvation. (F) P-body formation (red) after amino acid starvation (EBSS) is dependent on available mRNA, as seen by treatment with CHX. Control cells were treated for 6 h in EBSS. CHX-treated cells were incubated with EBSS for 2 h and then CHX was added for another 4 h. Scale bars: 20 μm.

Journal of Cell Science (2014) 127, 4443–4456 doi:10.1242/jcs.152975

sequence (CFP–SKL). When transcription was induced by doxycycline for 6 h followed by amino acid starvation for 6 h, there was a reduction of 60% in the induced protein levels compared to cells that were not subjected to amino acid starvation (Fig. 1D), whereas mRNA levels did not change (supplementary material Fig. S1B).

Cells were incubated overnight with EBSS in order to examine the effects of prolonged incubation under amino acid starvation conditions, and were found to be viable and to contain very high numbers of P-bodies as compared to untreated cells (Fig. 1B,E). Addition of serum to the EBSS medium did not reduce the number of P-bodies, whereas the addition of essential amino acids reversed the EBSS starvation effect (supplementary material Fig. S1C). Finally, because amino acid starvation enhances LC3 formation, a marker for autophagosomes (Ni et al., 2011), the possible interaction between P-body formation and autophagosomes was examined. Although we could confirm P-body formation and accumulation of LC3-marked autophagosomes during amino acid starvation and additional autophagosome-inducing treatments, there was no spatial connection between the two structures (supplementary material Fig. S2).

We next examined whether the increase in P-body assembly during amino acid starvation required a pool of free cytoplasmic mRNAs. We have previously demonstrated that inhibition of translation elongation using cycloheximide, a treatment that constrains mRNA to polysomes and thereby leads to reduction in the free cytoplasmic mRNA pool, results in P-body disassembly (Aizer et al., 2008). Fig. 1B,F shows that EBSS amino acid starvation (2 h) followed by cycloheximide plus EBSS treatment (4 h) resulted in complete P-body disassembly and in the dispersal of P-body protein components in the cytoplasm. Given that under these conditions, EBSS treatment did not lead to P-body assembly, we suggest that P-body formation during amino acid starvation requires an available pool of free mRNA.

mRNAs localize to P-bodies during amino acid starvation

In order to examine the fate of mRNAs and P-bodies during amino acid starvation, we utilized three different gene systems producing specific mRNAs that can be fluorescently tagged in living cells. mRNA tagging is achieved by the presence of multiple MS2 sequence repeats that form repeated stem-loop structures in the 3′ untranslated region (UTR) of the studied mRNA. The MS2 stem-loops are then coated by the MS2 coat protein fused to YFP (YFP–MS2), thereby providing pronounced staining of the mRNAs (Bertrand et al., 1998; Fusco et al., 2003) (Fig. 2A). We are using a YFP–MS2 protein that contains a nuclear localization signal (NLS) and a nuclear export signal (NES), such that it is distributed equally and with low background in the nucleus and the cytoplasm (Mor et al., 2010). The three types of genes used herein were stably integrated in U2OS cells and were under inducible promoter transcriptional control.

The first cell system expressed a Cerulean-mini-dystrophin gene (Mor et al., 2010) (Fig. 2B). The cells were transiently co-transfected with the YFP–MS2 coat protein to label the mRNAs transcribed from this gene, and with RFP–Dcp1b for following P-bodies in living cells (Aizer et al., 2008). Ponasterone A (PonA) was added to the cells for transcriptional activation of the gene. The YFP–MS2 label allows the observation of the active gene locus in the nucleus, as well as the cellular mRNAs transcribed from the gene. mRNA accumulation in P-bodies is infrequently observed under normal conditions (supplementary material Movie 1). However, when the cells were amino acid starved by EBSS treatment for 4 h, YFP–MS2 labeled mRNAs were easily detected in P-bodies (Fig. 2C; supplementary material Movies 2 and 3). The YFP–MS2 signal observed in the P-bodies was not due to non-specific accumulation of the free YFP–MS2 protein, as verified in cells subjected to amino acid starvation for 4 h but without PonA transcriptional activation (Fig. 2D; supplementary material Movie 4).

To verify that mRNA was indeed found within P-bodies independently of the YFP–MS2 protein tag, we performed RNA fluorescence *in situ* hybridization (FISH) using probes that target different regions of the mRNA in combination with anti-Hedls antibody immunofluorescence staining for P-body identification. A Cy3-labeled probe targeting the 5′-end of the Cerulean-mini-dystrophin transcript (the Cerulean region) and a Cy3-labeled probe against the 3′-end of the mRNA (MS2 region) (Fig. 3A) demonstrated the presence of the Cerulean-mini-dystrophin mRNAs in P-bodies during amino acid starvation (Fig. 3B,E).

Accumulation of other types of mRNA transcripts in P-bodies was also observed; Tet-inducible U2OS cell lines expressing either MS2-tagged CFP–β-actin transcripts (Fig. 3C–E; Ben-Ari et al., 2010) or β-globin–CFP transcripts (Brody et al., 2011) (supplementary material Fig. S3A) showed positive FISH signals for the different regions of the transcripts using FISH probes after doxycycline induction. These data, showing the 5′ and 3′ regions of the mRNAs within P-bodies, suggest that full-length mRNAs accumulate in P-bodies during amino acid starvation. To examine this further we performed RNA FISH with an oligo-d(T) probe that hybridizes with the poly(A) tails of mRNAs. However, after 4 h of amino acid starvation we could not detect a poly(A) signal within the P-bodies (supplementary material Fig. S3B), implying that mRNAs accumulating in P-bodies during amino acid starvation lacked the poly(A) tail. As a control, we show that in uninduced cells (no doxycycline), no MS2 FISH signal is observed in the cells (supplementary material Fig. S3C).

In order to assess the timing of the accumulation of mRNAs in P-bodies within the cell population in conjunction with the increase in P-body numbers during amino acid starvation, we counted P-body numbers and the percentage of P-bodies containing CFP–β-actin transcripts over time. In an untreated cell population, 18% of the cells displayed mRNAs inside P-bodies, as seen by RNA FISH (Fig. 3F, red line). There was a significant and gradual increase over time from the beginning of the translational stress, from 40% of cells harboring mRNAs inside P-bodies at 4 h, to 68% of the population doing so after 16 h of amino acid starvation. A similar quantification with the Cerulean-mini-dystrophin transcripts showed that after 16 h of amino acid starvation, 53% of the cell population contained mRNA in P-bodies (data not shown). This coincided with an elevation in the number of P-bodies in the same cells (Fig. 3F, gray bars). Taken together, this shows that although mRNAs are detectable in P-bodies in only a small number of cells under untreated conditions, after amino acid starvation the proportion of cells with mRNA in P-bodies is highly elevated, in addition to there being many more P-bodies per cell. The accumulation of mRNA in P-bodies was also followed in living cells using the CFP–β-actin-MS2 transcripts. Cells were transcriptionally induced with doxycycline for 6–8 h and then incubated under amino acid starvation conditions. Fig. 3G and supplementary material Movie 5 show that there was an increase in P-body numbers and in CFP–β-actin-MS2 mRNAs in P-bodies after several hours of stress. The initiation of mRNA accumulation in P-bodies could already be detected after 1 h of treatment.

Journal of Cell Science (2014) 127, 4443–4456 doi:10.1242/jcs.152975

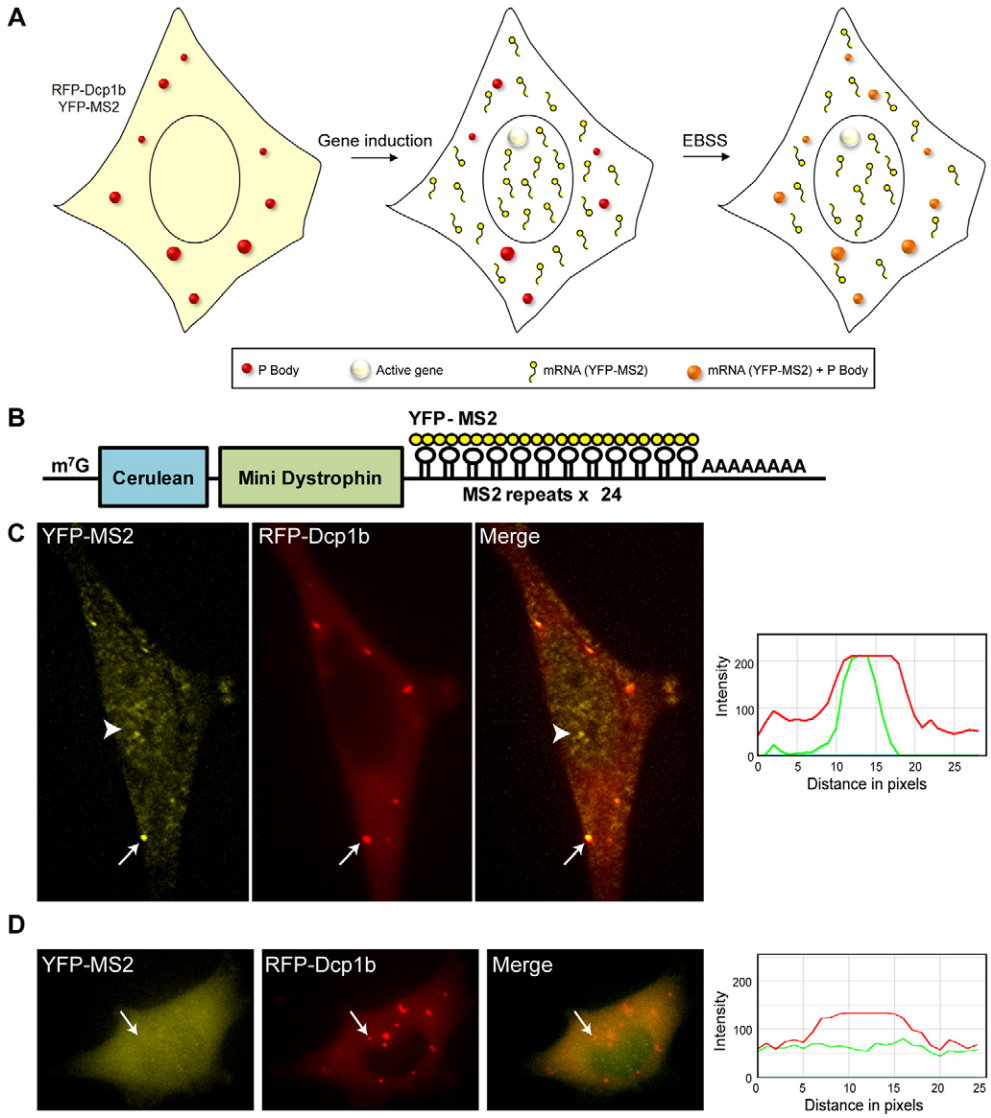

Fig. 2. mRNAs accumulate in P-bodies during amino acid starvation. (A) Schematic representation of the expected phenotype of YFP–MS2-tagged mRNAs and RFP–Dcp1b-labeled P-bodies (PBs) during gene induction and after amino acid starvation (EBSS medium). (B) Scheme showing the structure of the Cerulean-mini-dystrophin-MS2 mRNA and the region detected by the YFP–MS2 protein tag (yellow circles). (C) Frames from supplementary material Movie 2 showing an EBSS-treated cell expressing the Cerulean-mini-dystrophin mRNA (YFP–MS2, yellow) transfected with RFP–Dcp1b (red) and transcriptionally induced with PonA. Colocalization is plotted as intensity versus distance (green, mRNA; red, Dcp1b). The arrow indicates colocalization in the plotted area. The arrowhead indicates the active transcription site seen only with YFP–MS2. (D) Frames from supplementary material Movie 4 of an EBSS-treated transcriptionally uninduced cell expressing YFP–MS2 (without PonA activation) and transfected with RFP–Dcp1b. There is no colocalization between the two channels. The arrow indicates the plotted area.

Quantitative analysis of mRNA inside P-bodies

The number of mRNAs that can accumulate within P-bodies is unknown, particularly because it is difficult to detect mRNAs in P-bodies under normal conditions in mammalian cells (Fig. 3F). We therefore performed a quantification experiment on cells expressing the CFP–β-actin-MS2 transcripts and counted the number of mRNAs present in P-bodies relative to the total CFP–β-actin-MS2 mRNA in the cytoplasm, in untreated and in amino acid starved cells.

The quantification procedure was based on a previously described protocol for single mRNA analysis (Yunger et al., 2010; Yunger et al., 2013). 3D volumes of cells expressing the CFP–β-actin-MS2 gene that underwent RNA FISH with a probe against the MS2 region, were acquired. The *z*-stacks were deconvolved to provide high resolution detection of the cellular mRNAs. The nuclear volume was imaged separately in the Hoechst channel and subtracted from the analysis in order to obtain cytoplasmic values. The fluorescence intensity of single CFP–β-actin-MS2 mRNA molecules in the cytoplasm was measured. It was obvious that the total fluorescence intensity of the mRNAs within P-bodies was usually stronger than the single mRNAs, and therefore the fluorescence value of a single cytoplasmic mRNA was used to calculate the number of mRNAs harbored in P-bodies.

In an untreated population of cells we identified cells containing two to seven P-bodies per cell that had mRNA signal within them. In comparison, overnight amino acid starved cells had between 5 and 15 P-bodies per cell that contained mRNAs. Fig. 4A (left) shows the quantification of an untreated cell with five P-bodies that contain 0, 2 or 3 CFP–β-actin-MS2 mRNA transcripts. In comparison, Fig. 4A (right) shows quantification in an amino acid starved cell containing 15 P-bodies harboring from 0 to 10 β-actin-MS2 mRNA transcripts each. A gradual enrichment of mRNAs within P-bodies was seen from 6 h of amino acid starvation to overnight starvation. A steady state of mRNA accumulation in P-bodies was seen after overnight (Fig. 4B). The percentage of CFP–β-actin-MS2 mRNAs assembled in P-bodies, from the total of cytoplasmic CFP–β-actin-MS2 mRNAs, is shown for untreated cells and the two time points of amino acid starvation (Fig. 4C). In untreated cells, the P-body-associated mRNAs ranged between 1 to 13% of the total cytoplasmic CFP–β-actin-MS2 mRNA. By contrast, in amino acid starved cells this value ranged between 9 and 43% (Fig. 4C). Supplementary material Fig. S3D shows a histogram

Journal of Cell Science (2014) 127, 4443–4456 doi:10.1242/jcs.152975

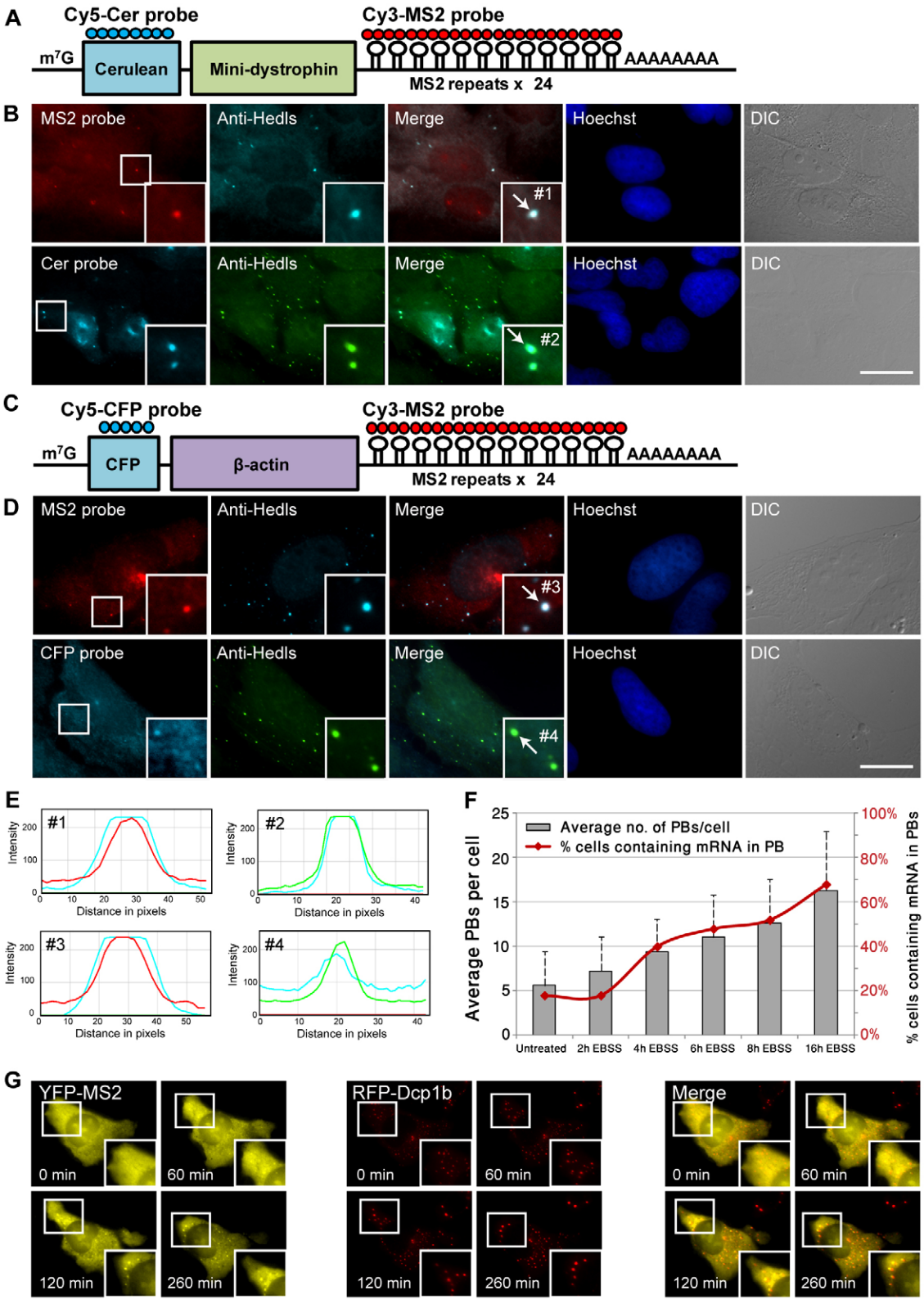

Fig. 3. See next page for legend.

plot of the distribution of the number of mRNAs inside P-bodies in the cells. In summary, under stress conditions, up to 40% of the total cytoplasmic CFP–β-actin-MS2 transcripts translocated to P-bodies.

P-body-associated mRNAs exhibit low exchange kinetics

We next examined the internal dynamics of the P-bodies components and the dynamics of the mRNAs localized in P-bodies, and whether the mRNAs might be exchanging with the

Journal of Cell Science (2014) 127, 4443–4456 doi:10.1242/jcs.152975

Fig. 3. mRNAs are observed in P-bodies during amino acid starvation. (A) Scheme showing the structure of the Cerulean-mini-dystrophin-MS2 mRNA and the region detected by the CFP probe (Cerulean region, cyan circles) and the MS2 probe (red circles). (B) Cells were transcriptionally activated by PonA, and EBSS was added overnight. Top, RNA FISH signal of the MS2 probe to the 3′UTR of the mRNA (red) and Hedls immunofluorescence (cyan) for P-body detection. Bottom, RNA FISH signal of the Cer probe to the 5′ region of the mRNA (cyan) and Hedls immunofluorescence (green). Arrows in boxed areas indicate colocalization in the areas plotted in E. (C) Scheme showing the structure of the CFP–β-actin-MS2 mRNA and the region detected by the CFP probe (cyan circles) and the MS2 probe (red circles). (D) Cells were transcriptionally activated by doxycycline, and EBSS was added overnight. Top, RNA FISH signal of the MS2 probe to the 3′UTR of the mRNA (red) and Hedls immunofluorescence (cyan) for P-body detection. Bottom, RNA FISH signal of the CFP probe to the 5′ region of the mRNA (cyan) and Hedls immunofluorescence (green). Arrows in boxed areas indicate colocalization in the areas plotted in E. Scale bars: 20 μm. (E) Colocalization is plotted as intensity versus distance according to the arrow numbers and channel colors in B and D. (F) Left *y*-axis, count of the number of endogenous P-bodies in EBSS-treated U2OS cells (gray bars, $n=51$ cells for each time point; mean±s.d.). Right *y*-axis, percentage of cells containing P-bodies with an mRNA signal (by RNA FISH) during amino acid starvation and over time (red line, $n=50$ cells). (G) Frames from supplementary material Movie 5 showing the accumulation of mRNA in P-bodies in real-time, in cells expressing the CFP–β-actin-MS2 mRNA (YFP–MS2, yellow) transfected with RFP–Dcp1b (red). Insets at the bottom right show a magnification of the boxed areas.

cytoplasmic pool during amino acid starvation. To determine the flux of protein or mRNA entering and possibly exiting P-bodies, we performed fluorescence recovery after photobleaching (FRAP) experiments on Dcp1a and Dcp2 proteins, and on CFP–β-actin-MS2 mRNAs tagged with YFP–MS2. Full recovery of the YFP–MS2 signal would be indicative of exchange and entry of new mRNAs into P-bodies, whereas partial recovery would indicate that some of these mRNAs are residing in P-bodies for some time.

FRAP of the Dcp1a or Dcp2 proteins in P-bodies of untreated cells and amino acid starved cells resulted in similar recovery rates (Fig. 5A; statistical analysis in supplementary material Fig. S4A–C), suggesting that association and dissociation rates of the protein components were not changing upon stress, and that the assembly of larger P-bodies might be due to the addition of the mRNA component within them. Photobleaching of YFP–MS2-tagged CFP–β-actin-MS2 mRNAs that localized in P-bodies without treatment (cells were co-transfected with YFP–MS2 coat protein and CFP–Dcp1b; note that CFP–β-actin protein accumulates very slowly and does not interfere with CFP–Dcp1b in P-bodies), showed incomplete YFP–MS2 recovery rates with a substantial immobile mRNA fraction within the P-bodies (~40%) (Fig. 5B,C). By contrast, after overnight amino acid starvation YFP–MS2 recovery was even slower showing an increase in the immobile mRNA fraction, meaning that 60% of the P-body-associated mRNAs were not exchanging with the cytosolic mRNA fraction (Fig. 5B,C; supplementary material Fig. S4D and Movie 6). This trend of a stationary mRNA population continued for more than 20 min of recovery (data not shown). Supplementary material Fig. S4G shows similar slow recovery rate results for the FRAP experiments with the Cerulean-mini-dystrophin-MS2 mRNAs during a long amino acid starvation. Taken together, this analysis suggests (1) that a notable stationary or stored fraction of mRNAs localizing to P-bodies is obtained under prolonged translational stress, and (2) that a slow exchanging or stored mRNA population also exists under unstressed conditions.

mRNA clearance from P-bodies after stress

The mRNAs accumulated in P-bodies for a long period during amino acid starvation. We next followed their fate after release from the stress. Time-lapse imaging was performed on stressed cells released from stress by the addition of amino acids into the medium. Cells expressing Cerulean-mini-dystrophin-MS2 and YFP–MS2-tagged mRNAs were transfected with RFP–Dcp1b for the co-detection of P-bodies, and were incubated overnight with EBSS medium. The Cerulean-mini-dystrophin-MS2 mRNAs were detected in P-bodies after this treatment. Regular DMEM medium and serum were then applied to the amino-acid-starved cells, and cells were imaged for several hours. Fig. 6 and supplementary material Movie 7 show that P-body numbers declined after release from starvation, in conjunction with a notable reduction in P-body-associated mRNAs. Most of the mRNA signal in P-bodies had cleared by 40 min and was completely gone by 100 min. These results were also observed in the CFP–β-actin-MS2 cell line as (data not shown). Counting of P-body numbers confirmed that the decrease after starvation release was due to the addition of amino acids and not serum (supplementary material Fig. S1C,D). These data could suggest that the mRNAs localized within P-bodies during translational stress are not immediately degraded but rather stored until cell recovery. After release from stress it would seem likely that some of the mRNAs are degraded because they lack poly(A) tails.

Some mRNAs localizing to P-bodies are removed by a Dcp2-dependent decay pathway

In light of the above conclusions, we wished to detect a P-body-associated mRNA population that is dependent on decay. Under both untreated and EBSS-treated conditions, the incomplete mRNA FRAP recovery curves meant that there is a population of mRNAs in P-bodies that is not exchanging for many minutes, as well as a population that is slowly exchanging. The latter could be attributed to either a steady state of flux of mRNA in and out of P-bodies (i.e. stored mRNAs), or could be due to degradation activity within the P-body that makes room for the entry of new mRNAs. To examine this issue we knocked down the levels of the Dcp2 decapping protein. Unlike knockdown of many other P-body components, Dcp2 knockdown does not lead to the disassembly of P-bodies, and so we could continue to study the P-body–mRNA association under these conditions. In addition, the levels of Dcp2 in P-bodies are limited as it is a core component, and has been found to be non-exchanging by FRAP experiments (Fig. 5A; Aizer et al., 2008). Given that the slow exchange dynamics of the mRNA might result from the long EBSS treatment (Fig. 5B), we examined the kinetics of CFP–β-actin-MS2 mRNAs in P-bodies after 4 h of EBSS treatment, because a highly detectable accumulation of mRNAs in P-bodies was already found at this time (Fig. 2E; Fig. 3F). Using siRNA against Dcp2, we reduced Dcp2 levels (Fig. 7A) and found that mRNAs continued to accumulate in P-bodies under both normal and amino acid starvation conditions (40% exchanging, 60% retained; Fig. 7B,C). However, it can also be seen that once Dcp2 levels were reduced, the kinetics of the mRNA FRAP recovery curves became significantly slower, reaching ~20% recovery only (Fig. 7B,C and supplementary material Movie 8) compared to use of a scrambled siRNA that did not affect the FRAP recovery rates. This meant that a larger mRNA population (~80%) was retained within the P-bodies when Dcp2 was depleted. Indeed, qPCR measurements of the levels of CFP–β-actin-MS2 under actinomycin D treatment (thus preventing the

Journal of Cell Science (2014) 127, 4443–4456 doi:10.1242/jcs.152975

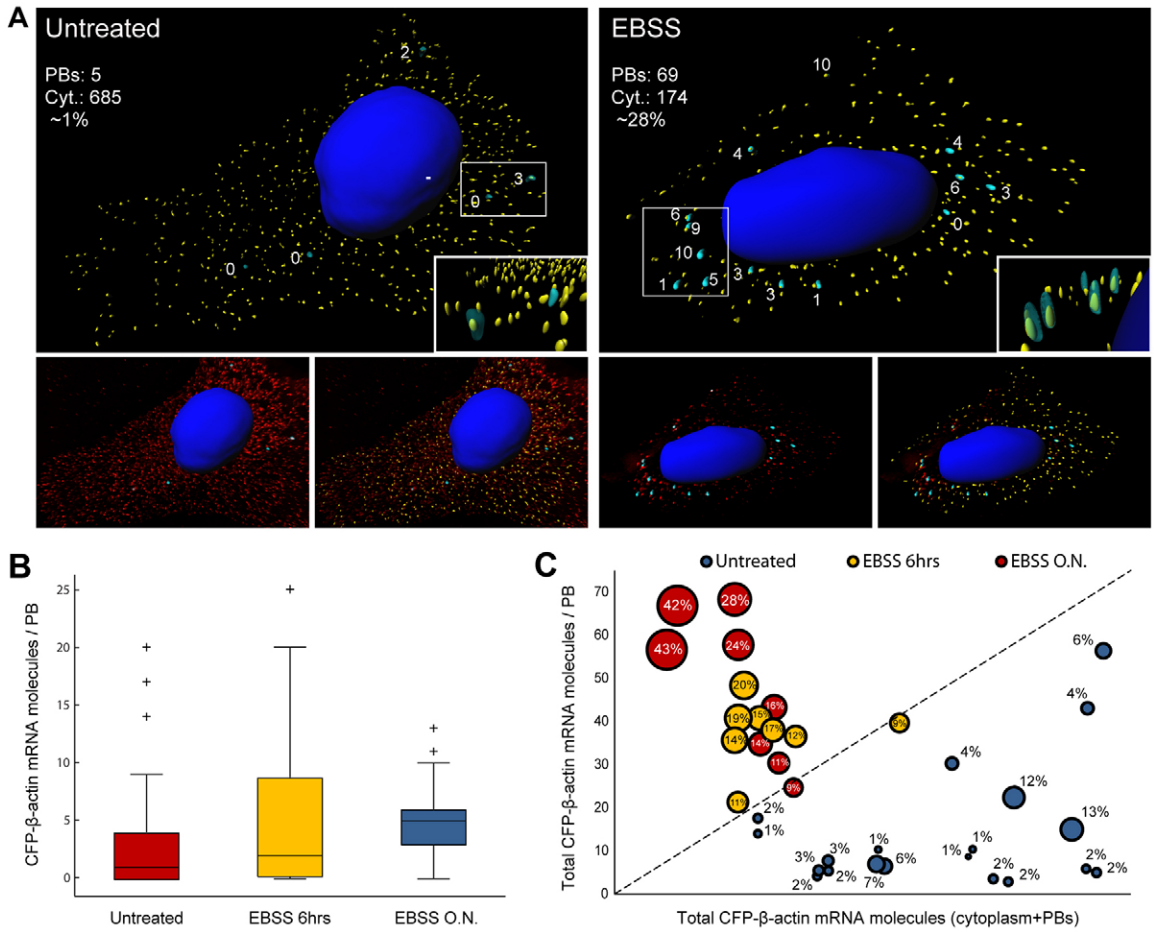

Fig. 4. Quantitative analysis of mRNA numbers inside P-bodies relative to cytoplasmic mRNAs. (A) 3D projection of the whole cell volume for CFP–β-actin-MS2 mRNA (mRNA surfaces, yellow) distribution in an untreated cell (left) and an EBSS-treated cell (right). The numbers above certain P-bodies (PBs) (cyan) indicate the number of transcripts within the P-body. On the left are noted the number of P-bodies in the cell, the number of cytoplasmic CFP–β-actin-MS2 mRNAs (Cyt.) and the percentage of CFP–β-actin-MS2 mRNAs within the P-bodies. Insets at the bottom right show a magnification of the boxed areas. The lower panels demonstrate, for each large image above, the 3D mRNA distribution (red) in the cytoplasm with (left) P-body surfaces (cyan) and (right) P-body surfaces (cyan) and mRNA surfaces (yellow). (B) A boxplot representing the number of CFP–β-actin-MS2 mRNAs inside P-bodies in untreated versus EBSS-treated cells [$n=51$ P-bodies (untreated), 35 P-bodies (6 h EBSS) and 39 P-bodies (overnight EBSS)]. The median is indicated by the black line, the box represents the interquartile range and the whiskers represent the maximum and minimum values. (C) mRNA accumulates in P-bodies in EBSS-treated cells. Each dot denotes a cell: blue, untreated; yellow, 6 h EBSS; red, overnight EBSS. The size of the dots represents the percentages of CFP–β-actin-MS2 mRNA in P-bodies compared with the total cytoplasmic CFP–β-actin-MS2 mRNA. The *y*-axis represents the total number of CFP–β-actin-MS2 mRNAs in the P-bodies, and the *x*-axis represents the total number of CFP–β-actin-MS2 mRNAs in the cytoplasm including P-bodies.

addition of new mRNAs), showed that when Dcp2 levels were reduced there was less decay of the mRNA (Fig. 7D). Moreover, RNA FISH quantification of mRNA levels in P-bodies under Dcp2-knockdown conditions showed a significant increase in the mRNA population within the P-bodies (Fig. 7E), from an average of 7±6 mRNAs per P-body in scrambled siRNA-treated cells, to 14±8 mRNAs per P-body in Dcp2-knockdown cells (mean±s.d., $n=74$ and 62 P-bodies, respectively, $P<0.001$). Taken together, these findings imply that Dcp2 normally plays a role in mRNA exchange within P-bodies (and also during amino acid starvation), thus leading to turnover of some of the mRNA in the P-bodies (a third of the exchanging population) and allowing new mRNAs to enter. When Dcp2 was absent, mRNA decay was less prominent and more mRNAs were stored in the P-bodies. The data from the slow FRAP recovery curves suggest that mRNAs can accumulate in P-bodies for long periods and that a portion of this population is constantly removed by a Dcp2-dependent decay pathway.

DISCUSSION

P-bodies harbor proteins that function in mRNA decay and translation repression. They are easily detectable in cells, and are dynamic structures associated with the cytoskeleton (Sweet et al., 2007; Aizer et al., 2008; Gallina et al., 2013). P-bodies can assemble or disassemble in accordance to cell cycle stage or in response to stress (Kedersha et al., 2005; Teixeira et al., 2005; Aizer et al., 2008; Aizer et al., 2013). In this study, we demonstrated that amino acid starvation leads to an increase in P-body numbers and to the detectable accumulation of mRNAs in P-bodies. Our data suggest that an available cytoplasmic mRNA pool is required for the enhanced P-body assembly during amino acid starvation, in accordance with previous studies demonstrating that the dynamic structure of P-body complexes depends on an available non-translating cytoplasmic mRNA pool (Andrei et al., 2005; Liu et al., 2005; Pillai et al., 2005; Teixeira et al., 2005).

Journal of Cell Science (2014) 127, 4443–4456 doi:10.1242/jcs.152975

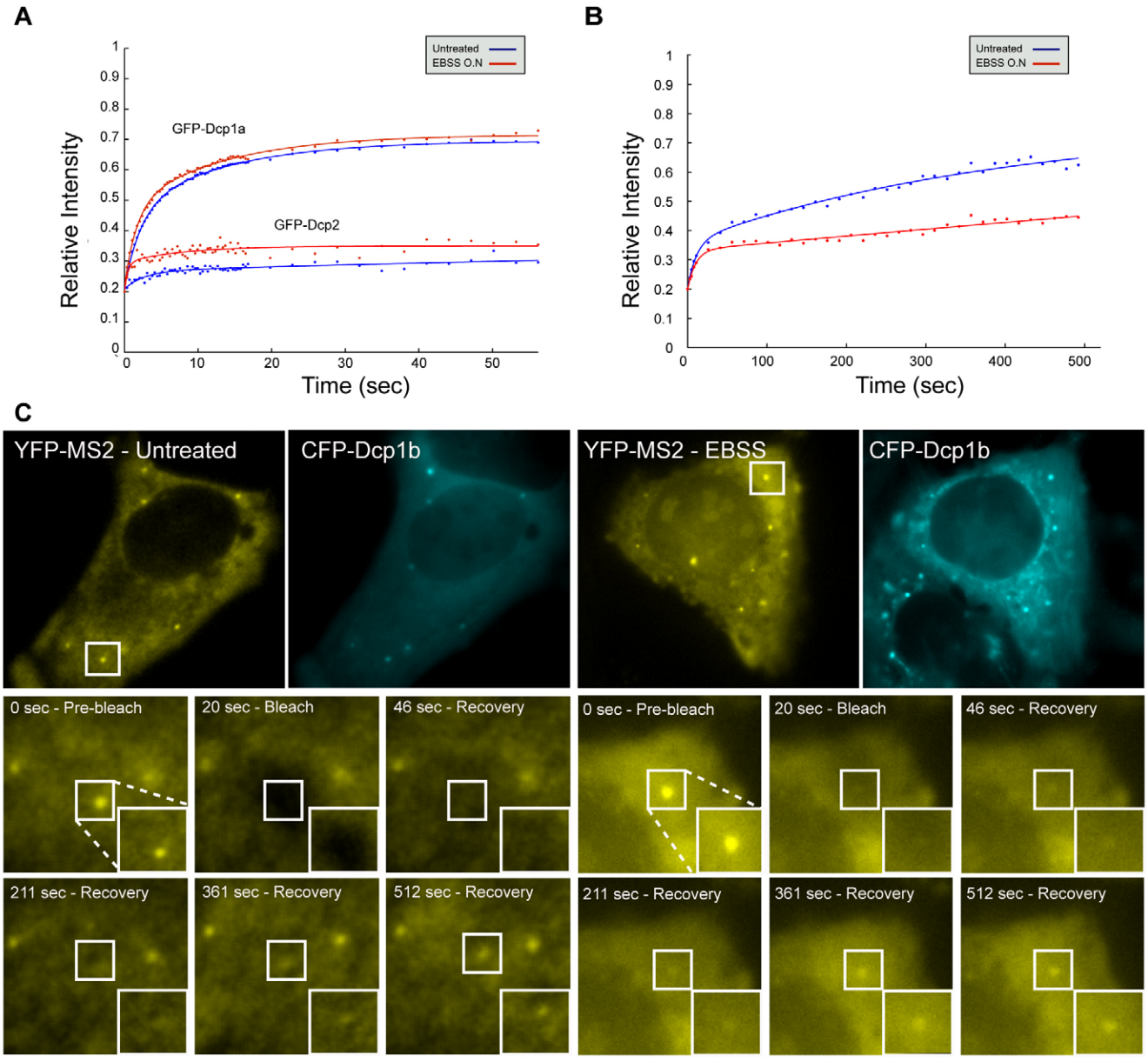

Fig. 5. P-body-associated mRNAs exhibit slow exchange kinetics. (A) Dynamics of P-body protein components Dcp1a (upper plots, $t_{1/2}$: untreated 3.2 s, EBSS 2.6 s) and Dcp2 (bottom plots) in untreated cells and EBSS-treated cells (4 h), presented as an averaged data plot of FRAP recovery curves (n=20). (B) Dynamics of YFP–MS2-tagged CFP–β-actin mRNA in P-bodies. Data are presented as an averaged data plot of FRAP recovery curves in untreated and 16 h EBSS-treated cells (n=11 P-bodies and 10 P-bodies respectively). (C) Colocalization of mRNA labeled by YFP–MS2 (yellow) and P-bodies marked by CFP–Dcp1a (cyan) in living untreated and EBSS-treated cells for 16 h. Bottom, frames showing one pre-bleach frame, the bleach of the YFP–MS2 signal in one P-body, and frames following the recovery of signal over time.

Yeast studies have shown that translation inhibition can be caused by glucose deprivation or amino acid starvation (Brengues and Parker, 2007; Hoyle et al., 2007). In this study, we established a relationship between translational activity and mRNA assembly in P-bodies. When cells were starved for amino acids, we detected a significant increase in the percentage of the three different mRNA species we tested within P-bodies, accompanied by an increase in P-body numbers. This effect was relieved when essential amino acids were added back to the medium. The connection between mRNA accumulation in P-bodies and translational stress or repression has been observed in several systems, and implies that there is a dynamic process that senses the translational state of the cell. It is now well established that mRNAs targeted for translational repression by miRNAs can accumulate in mammalian P-bodies, as first demonstrated for the let-7 miRNA (Liu et al., 2005; Pillai et al., 2005). Another example is ARE-mRNAs, which undergo translational silencing and rapid turnover. They contain AU-rich elements (AREs) in their 3′UTRs and have been observed in P-bodies. This localization is enhanced when decay factors were limiting, thereby suggesting that this is a mechanism for ARE-mRNA sequestration in P-bodies when mRNA decay is deficient (Franks and Lykke-Andersen, 2007). Glucose starvation causes an increase in P-body numbers and exit of ARE-mRNA from P-bodies through a RhoA-dependent

Journal of Cell Science (2014) 127, 4443–4456 doi:10.1242/jcs.152975

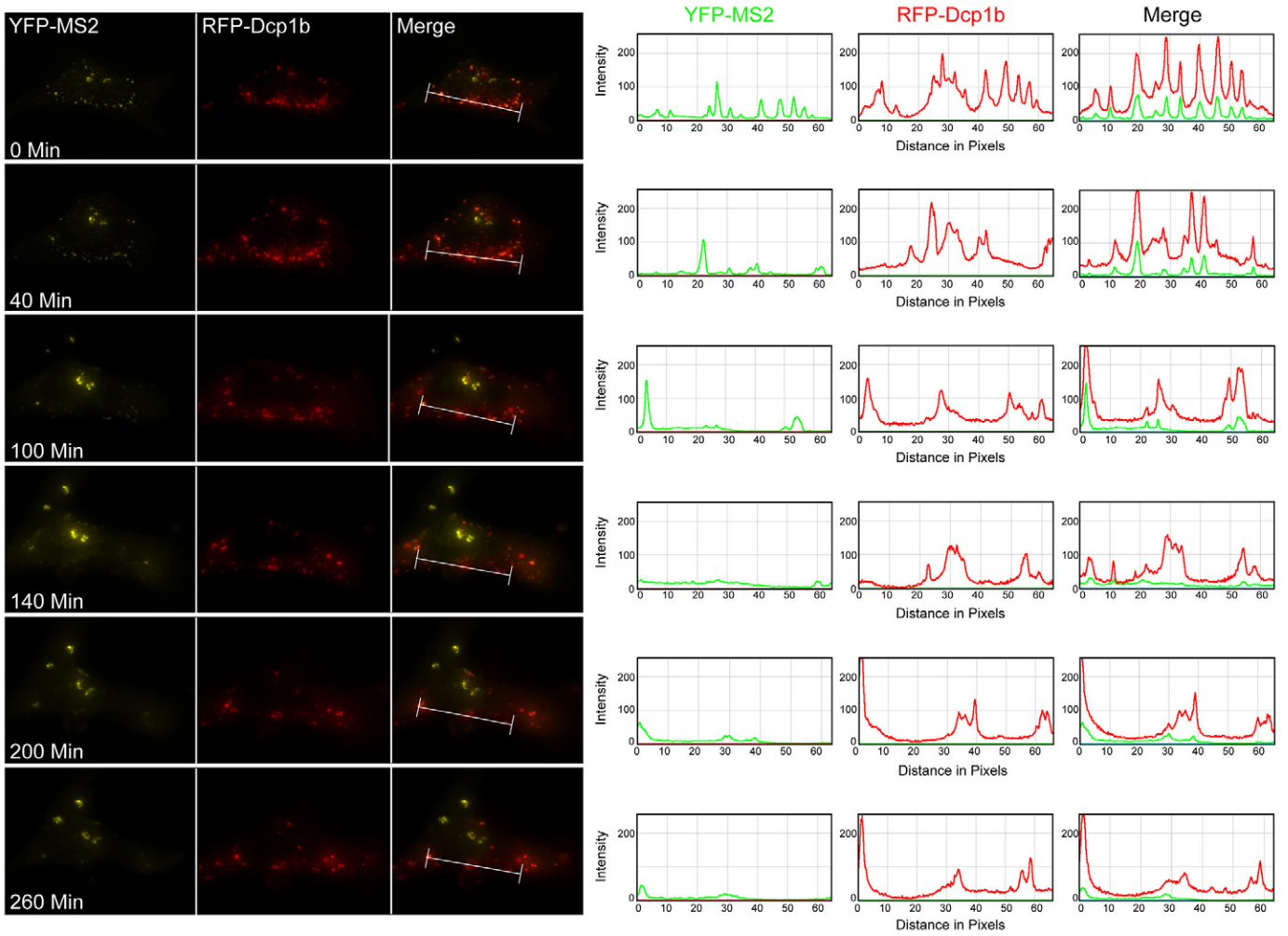

Fig. 6. mRNA clearance from P-bodies after release of stress. Cells expressing RFP–Dcp1b (red) were transcriptionally activated by PonA to express the Cerulean-mini-dystrophin transcript, tagged by YFP–MS2 (yellow). EBSS was added for 16 h. To release from the stress, DMEM containing FBS and glutamine were added for the indicated times. Colocalization is plotted as the intensity versus distance. Green is the mRNA and red is the P-body. At first, high colocalization between the P-bodies and mRNAs is observed (right-hand red and green plots). As cells are released from stress, this correlation disappears and P-body numbers decrease. The line indicates the plotted area.

pathway (Franks and Lykke-Andersen, 2007). Recently, the distribution of several mRNAs in *Drosophila* P-bodies has been examined at high resolution and it was demonstrated that P-bodies were involved in translational regulation of transcripts in a developing organism (Weil et al., 2012). An opposite example also exists. Dynamic exchange of mRNA between P-bodies and polysomes was observed for the cationic amino acid transporter 1 (CAT-1) mRNA in Huh7 cells, which are known to regulate CAT-1 levels using inhibition mediated by the miRNA miR-122 (Bhattacharyya et al., 2006), showing that certain mRNAs are capable of initiating translation during amino acid starvation.

Native mRNA transcripts do not typically accumulate in P-bodies, and only 1% of total mRNA has been estimated to interact with P-bodies in mammalian cells under unperturbed conditions (Stöhr et al., 2006; Franks and Lykke-Andersen, 2007; Zurla et al., 2011). In order to analyze the association of mRNAs with P-bodies in real-time, an mRNA system that can be tracked in living cells was designed and allowed us to track mRNA dynamics in P-bodies. The MS2 system allowed us to visualize β-actin, dystrophin and β-globin mRNA transcripts in single living human cells and to quantify mRNA dynamics in P-bodies before and after amino acid starvation. Using these cells for RNA FISH provided high-resolution information about the mRNA distribution in the cytoplasm and P-bodies, and enabled the counting of the transcripts. We first showed that the percentage of P-bodies with detectable mRNAs increased from ∼20% in untreated cells to ∼70% during amino acid starvation. Counting the number of mRNA transcripts inside P-bodies under unperturbed conditions and during amino acid starvation revealed a dramatic increase from the very few mRNAs detected in P-bodies without any treatment, up to 40% of the detected mRNA population when cells were starved.

The relative percentage of an mRNA population in P-bodies was previously estimated for the hypoxia-inducible factor-1α (HIF-1α) mRNA (Carbonaro et al., 2011). This transcript is associated with the microtubule cytoskeleton, where it is actively translated. Disruption of the microtubule network caused the re-localization of HIF-1α to P-bodies in HeLa cells. qRT-PCR quantification showed that in untreated cells only 9% of cellular HIF-1α mRNA associated with Argonaute a P-body marker,

Journal of Cell Science (2014) 127, 4443–4456 doi:10.1242/jcs.152975

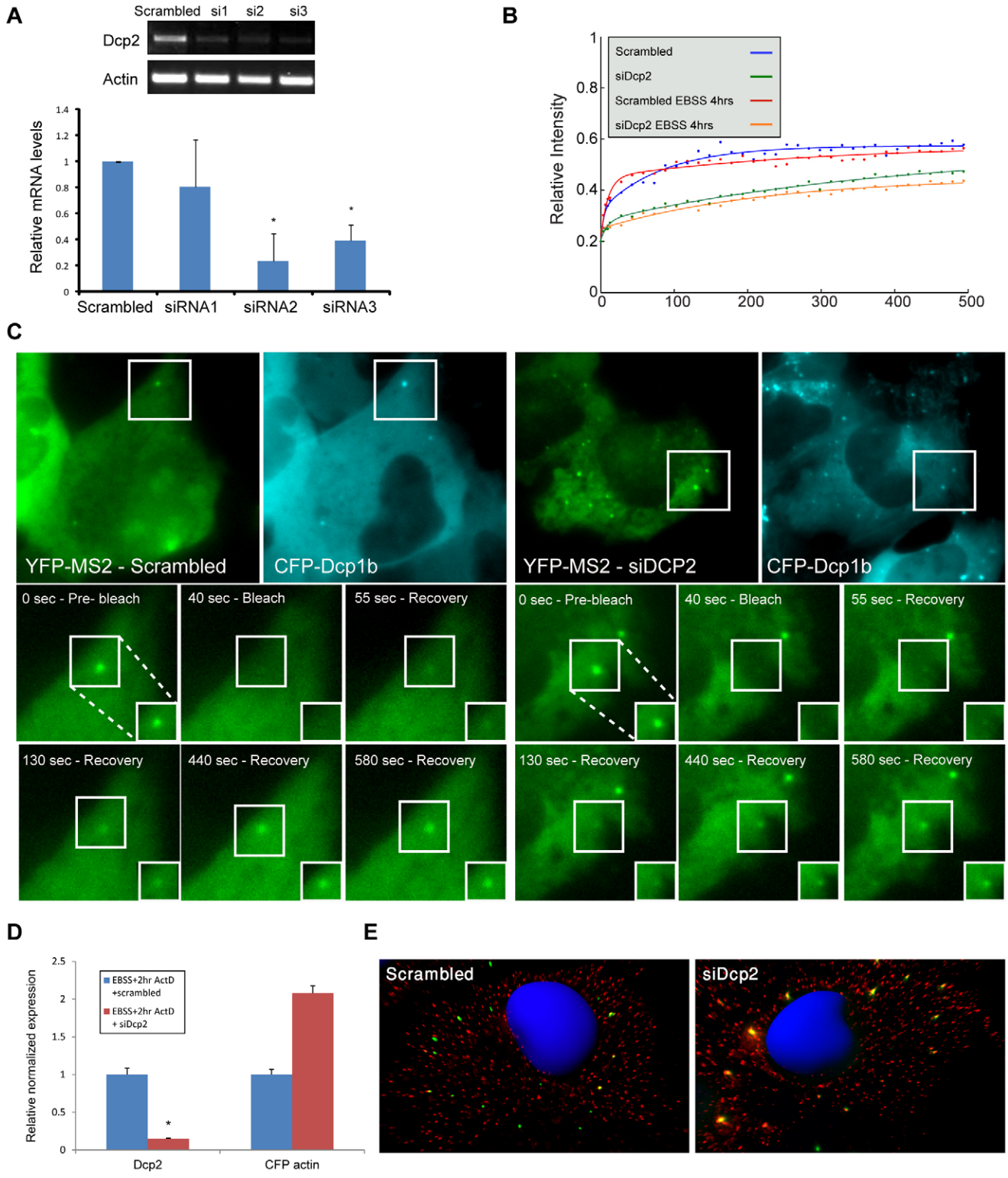

Fig. 7. Knockdown of Dcp2 slows mRNA exchange dynamics in P-bodies. (A) Dcp2 mRNA levels were reduced by siRNA (n=3, mean±s.d., *P<0.05). A scrambled siRNA was used as a control. siRNA no.2 was used for FRAP experiments. (B) Dynamics of YFP–MS2-tagged CFP–β-actin mRNA in P-bodies in untreated and EBSS-treated cells under Dcp2-knockdown conditions. The measured cells were: untreated cells that received a scrambled siRNA sequence (blue), untreated cells with siRNA to Dcp2 (green), 4 h EBSS-treated cells with the scrambled sequence (red), and 4 h EBSS-treated cells with Dcp2 knockdown (orange) (n=15 per treatment). (C) Colocalization of mRNA labeled by YFP–MS2 (green) and P-bodies marked by CFP–Dcp1a (cyan) in living untreated cells and after Dcp2 knockdown. Bottom, frames showing one pre-bleach frame, the bleach of the YFP–MS2 signal in one P-body (red circle) and frames following the recovery of signal over time. (D) qPCR showing that after Dcp2 knockdown (left) there is a rise in cellular CFP–β-actin mRNA levels (right) in EBSS-treated cells, under actinomycin D (ActD, 5 μg/ml, 2 h) transcriptional inhibition conditions. (E) 3D projections of RNA FISH images from EBSS-treated cells with a Cy3–MS2 probe against the CFP–β-actin mRNA (red) together with immunofluorescence to Hedls (green), showing high levels of the mRNA in P-bodies after Dcp2 knockdown (right) versus scrambled siRNA-treated cells (left).

Journal of Cell Science (2014) 127, 4443–4456 doi:10.1242/jcs.152975

whereas this fraction increased to 70% when Taxol was administered. A 20% overlap between HIF-1α and P-bodies was observed by fluorescence microscopy after 1 h of treatment. After drug release, the HIF-1α mRNAs could return to the translating pool.

The RNA FISH analysis we performed showed that, although FISH probes could easily detect the 5′ and 3′ regions of the studied mRNAs within P-bodies, poly(A) tails were undetectable. Indeed, P-bodies do not contain PABP-1 (Kedersha et al., 2005), suggesting that mRNA in P-bodies is deadenylated. P-bodies contain four deadenylation nucleases (Pan2, Pan3, Ccr4 and Caf1) and cannot form if deadenylation is impaired as observed in yeast and mouse cells (Sheth and Parker, 2003; Cougot et al., 2004; Andrei et al., 2005; Zheng et al., 2008). It has been suggested that the first phase of deadenylation involves the dissociation of PABP from the transcript, and this occurs before messenger ribonucleoproteins (mRNPs) enter P-bodies (Zheng et al., 2008).

Given that the FISH experiments demonstrated that most of the mRNAs tested could be detected in P-bodies but without their poly(A) tails, it was interesting to examine transcript fate with regard to storage and decay. This was performed using FRAP experiments. We hypothesized that if the mRNAs were being degraded in P-bodies, then a dynamic exchange with the cytoplasmic pool should be detected. FRAP recovery curves of mRNAs in P-bodies showed a gradual increase of the fluorescence signal after photobleaching indicating that these mRNAs were exchanging between the P-bodies and cytoplasm. These kinetics were dependent on Dcp2, suggesting that decay is playing a partial role in the exchange of mRNA from within P-bodies; when Dcp2 levels were reduced, there was a prominent reduction in the recovery rates. In addition, in comparison with previous FRAP measurements (Aizer et al., 2008; Aizer and Shav-Tal, 2008), there was no obvious change in the dynamics of P-body protein components due to the amino acid starvation, suggesting that the P-body structure is maintained under these conditions. qPCR measurements showed a reduction in the decay rates of the mRNA when Dcp2 was depleted (under actinomycin D treatment), which coincided with a quantifiable increase in mRNA population within the P-bodies when Dcp2 was depleted, showing that Dcp2 plays a role in mRNA decay in the P-body structure. Finally, when cells were imaged during the release from amino acid starvation, we found that the mRNA signal cleared out of P-bodies as the stress was released, suggesting that a significant portion of the mRNAs localized in P-bodies are not degraded but stored until cell recovery (Brengues et al., 2005; Bhattacharyya et al., 2006).

Taken together from a dynamic perspective, these data imply that the P-body-associated mRNAs are, at least partially, immobilized within P-bodies. These dynamics differ from measurements of mRNAs in stress granules using the RNA-binding protein CPEB1 and a MS2-tagged β-Gal reporter, which showed short residence times in stress granules with a time scale in the order of minutes. RNA FISH showed that β-Gal mRNA in stress granules represented only 9% of the total cytoplasmic β-Gal mRNA (Mollet et al., 2008). Rapid mRNA recovery rates as well as a small immobile mRNA fraction were also found in *Drosophila* cell stress granules formed under hypoxia conditions (van der Laan et al., 2012). The lack of poly(A) tails for mRNAs in P-bodies suggests that P-bodies play a role in mRNA decay. This might be the first prerequisite for an mRNA entering a P-body and hence the enrichment of deadenylases within this structure. Removal of the tail can lead to mRNA decay if the cellular conditions require this; however, mRNAs can pause in this state until a decision is made. The fact that mRNA turnover in P-bodies is not rapid, as observed by the FRAP analysis, together with the fact that there is an increase in the resident mRNAs when Dcp2 is lacking, suggests that deadenylation does not necessarily lead to decay and that deadenylation and decay occur independently. This strengthens the ‘mRNA cycle’ hypothesis proposed by Parker and colleagues, which suggests that mRNA in P-bodies can have different fates. Once mRNAs have encountered the decapping machinery they can either be directly degraded by the enzymes present in the P-body, aggregate into a P-body or undergo remodeling such that the degradation machinery is exchanged for translation initiation factors, thereby returning them to the translating pool (Decker and Parker, 2012). Several studies have shown evidence arguing that mRNA degradation occurs inside P-bodies. One of the main lines of evidence is that P-bodies contain many factors involved in mRNA decay (Kedersha et al., 2005). However, the high concentration of these enzymes in P-bodies does not necessarily imply that they are enzymatically active in mammalian cells at all times. In fact, it has been questioned whether mRNA decay or decapping actually takes place within P-bodies (Eulalio et al., 2007b). Our analysis has demonstrated the fate of different mRNA species inside P-bodies showing that part of the P-body-associated mRNA population very slowly exchanges with the cytoplasmic pool and remains within P-bodies for many minutes, implying a role for P-bodies as both a decay site and a storage complex.

MATERIALS AND METHODS

Plasmid construction

For CFP–Dcp1a, the human Dcp1a open reading frame (ORF) was amplified by RT-PCR from U2OS total RNA, using primers, sense 5′-ATACTCGAGAGATGGAGGCGCTGAGTCGAGCT-3′ and antisense 5′-ATAGAATTCGTCAAAACAAGGATCTGCTGGTGA-3′, and subcloned into *Xho*I/*Eco*RI sites of peCFP-C1 (Clontech).

Cell culture and transfections

Human U2OS cells were maintained in low-glucose DMEM (Biological Industries, Beit-Haemek, Israel), human RKO cells were maintained in MEM-Eagle (Biological Industries), and MEF cells were maintained in high-glucose DMEM (Gibco) each supplemented with 10% fetal bovine serum (HyClone Laboratories, Logan, UT). For mRNA detection in P-bodies, different cell clones expressing MS2 transcripts were used: β-actin-MS2 (Ben-Ari et al., 2010), β-globin-MS2 (Brody et al., 2011) and Cerulean-mini-dystrophin-MS2 (Mor et al., 2010). For transient transfections, cells were transfected with 1–5 µg of plasmid DNA and 40 µg of sheared salmon sperm DNA (Sigma) when using electroporation (Gene Pulser Xcell, Bio-Rad). For lipososmal transfection, the PolyJet transfection reagent (SignaGem Laboratories, MD, USA) or Lipofectamin 2000 (Invitrogen, NY, USA) were used. In order to detect the mRNA transcripts in P-bodies of living cells, cells were co-transfected with the YFP–MS2 and RFP– or CFP–Dcp1 plasmids. Cells were induced to express the β-globin-MS2 or β-actin-MS2 by addition of 1 µg/ml doxycycline (Sigma). Cerulean-mini-dystrophin-MS2 transcripts were induced with 1 µg/ml Ponesterone A (Sigma). For EBSS starvation, cells were washed twice with 1× PBS and incubated with EBSS medium (Biological Industries) for 1–24 h as indicated. The final concentration for the cycloheximide treatment was 5 µg/ml. For autophagosome formation, cells were treated with 10 µM etoposide (Sigma), 10 nM thapsigargin (Alomone Labs, Jerusalem, Israel), or 10 µM MG132 (Merck\Calbiochem).

Immunofluorescence

Cells were grown on coverslips, washed with PBS and fixed for 20 min in 4% PFA. Cells were then permeabilized in 0.5% Triton X-100 for

3 min. After blocking, cells were immunostained for 1 h with a primary antibody, and after subsequent washes the cells were incubated for 1 h with secondary fluorescent antibodies. Primary antibodies used were mouse anti-hDcp1a (Abnova), mouse anti-Dcp1a and mouse anti-Hedls (Santa Cruz Biotechnology) antibodies. Secondary antibodies used were Alexa-Fluor-488, -594 or -647-labeled goat anti-mouse-IgG antibody (Invitrogen). Nuclei were counterstained with Hoechst 33342 and coverslips were mounted in mounting medium.

Western blotting

Cells were washed in cold PBS, and proteins were extracted in RIPA lysis buffer (50 mM Tris-HCl pH 8.0, 5 mM EDTA, 150 mM NaCl, 0.5% Nonidet P-40) containing 10 mM sodium fluoride, 1 mM sodium orthovanadate, protease inhibitor cocktail (Sigma), 2.8 µg/ml aprotinin and 1 mM PMSF, and placed on ice for 20–25 min. The resulting lysate was centrifuged at 10,621 ***g*** for 10 min at 4℃. 20–40 µg/µl of protein per lane was run on SDS-polyacrylamide gels and transferred onto a nitrocellulose membrane (0.45 µm). The membrane was blocked in 5% BSA, and then probed with a primary antibody for 2 h at room temperature, followed by incubation with horseradish peroxidase (HRP)-conjugated goat anti-rabbit- or mouse-IgG antibody (Sigma) for 1 h at room temperature. For a loading control, the blots were reblotted with an anti-α-tubulin antibody (Abcam). Immunoreactive bands were detected by the enhanced chemiluminescence kit (ECL, Pierce). Primary antibodies used were mouse anti-hDcp1a (Abnova), rabbit anti-Dcp2 (Abcam) and mouse anti-GFP (Roche) antibody.

RNA FISH

Cells expressing GFP-labeled P-bodies were grown on coverslips and fixed for 20 min in 4% paraformaldehyde, and overnight with 70% ethanol at 4℃. The next day, cells were washed with 1× PBS and treated for 4 min with 0.5% Triton X-100. Cells were washed with 1× PBS and incubated for 10 min in 40% formamide (4% SSC). Cells were hybridized overnight at 37℃ in a dark chamber in 40% formamide with specific fluorescently labeled (Cy3 or Cy5) DNA probes (~10 ng probe, 50-mer). The next day, cells were washed twice with 40% formamide for 15 min and then washed for two h with 1× PBS. For oligo-d(T) labeling, 15% formamide was used. Nuclei were counterstained with Hoechst 33342 and coverslips were mounted in mounting medium. The following probes were used: CFP/Cer, 5′-ATATAGACGTTGTGGCTGATGTAGTTGTACTCCAGCTTGTGCC-CCAGGATA-3′;

MS2-binding site: 5′-CTAGGCAATTAGGTACCTTAGGATCTA-ATGAACCCGGGAATACTGCAGAC-3′; and PolyA, an oligo(dT) probe. In some cases, immunofluorescence was performed after the RNA FISH using the standard protocol.

mRNA quantification

For quantification of the number of mRNAs in the P-bodies or in the total cell, we used our previously published protocol (Yunger et al., 2010; Yunger et al., 2013) in which the intensity of a single mRNA is determined and this value is used to calculate the number of mRNAs in each P-body. 3D stacks (0.1-µm steps, 101 planes) of the total volume of the cells were acquired from the RNA FISH experiments performed on the β-actin-MS2 cells. 3D stacks were also collected for the Hoechst and anti-Hedls antibody signals. The 3D stacks were deconvolved using the Huygens Essential software (Scientific Volume Imaging, Hilversum, The Netherlands), and then the nuclear region was subtracted from the whole-cell volume and the specific signals of cytoplasmic mRNPs with P-bodies were identified (Imaris, Bitplane, Saint Paul, MN). mRNA identification was performed by comparing to deconvolved stacks acquired from native U2OS cells that did not express the β-actin-MS2 transcripts. The latter served as controls for the background levels of non-specific fluorescence. No mRNAs were identified in control cells. The intensity for each cytoplasmic mRNA was measured in the cells using Imaris (Yunger et al., 2010). Then the single mRNA intensities were pooled and the frequency value of a single mRNA was calculated. The number of mRNAs associated with each P-body was obtained by dividing the sum of mRNA intensity in the P-bodies by the frequent value of a single mRNA.

Fluorescence microscopy, live-cell imaging and data analysis

Wide-field fluorescence images were obtained using the Cell^R system based on an Olympus IX81 fully motorized inverted microscope (60× PlanApo objective, 1.42 NA) fitted with an Orca-AG CCD camera (Hamamatsu) driven by the Cell^R software. Live-cell imaging was carried out using the Cell^R system with rapid wavelength switching. For time-lapse imaging, cells were plated on glass-bottomed tissue culture plates (MatTek, Ashland, MA) in medium containing 10% FBS at 37℃. The microscope is equipped with an incubator that includes temperature and CO_2 control (Life Imaging Services, Reinach, Switzerland). For long-term imaging, several cell positions were chosen and recorded by a motorized stage (Scan IM, Märzhäuser, Wetzlar-Steindorf, Germany). In these experiments, cells were typically imaged in 3D (four *z*-planes per time point) every 10 to 20 min, at 2–3.33-µm steps. For presentation of the movies, the 4D image sequences were transformed into a time sequence using the maximum projection option or manual selecting using the ImageJ software. 3D analysis was performed with the Imaris. Movie sequences were deconvolved using Huygens.

Fluorescence recovery after photobleaching

FRAP experiments were performed using a 3D-FRAP system (Photometrics) built on an Olympus IX81 microscope (636 Plan- Apo, 1.4 NA) equipped with an EM-CCD (Quant-EM, Roper), 491-nm lasers, a Lambda DG-4 light source (Sutter), XY&Z stages (Prior), and driven by MetaMorph software (Molecular Devices). Experiments were performed at 37℃ under 5% CO_2 using a live-cell chamber system (Tokai). For mRNA FRAP experiments, cells were imaged in the YFP channel for the detection of YFP–MS2 (mRNA) and in the CFP channel for the detection of CFP–Dcp1a (P-bodies). For each acquisition, at least nine z-slices were taken every 400 nm. The target P-body was bleached for 500 ms using the 491-nm laser. Six pre-bleach images were acquired. Post-bleach images were acquired at two time intervals. The first interval was taken for 1.5 s every 300 ms and the second interval was taken for 480 s every 15 s. FRAP experiments were analyzed using lab-written ImageJ macros previously described (Brody and Shav-Tal, 2011). All FRAP experiments in Figs 5 and 7 represent average recovery curves of many P-bodies in one experiment, and each experiment was performed at least twice.

The FRAP data was fitted with a double exponential model, $I(t)=\alpha_1 * \exp(-\tau_1 * t)+\alpha_2 * \exp(-\tau_2 * t)+c$ where $t=0$ is the moment right after the photbleaching. $t_{0.5}$ was defined as time where $I(t=t_{0.5})=\frac{I(t=\infty)}{2}$. In Fig. 5B, we measured a $t_{0.5}$ of 143 s for the recovery rate of P-body in untreated cells using an exponential fit with $r_{square}=0.988$. P-body recovery rate in cells treated with EBSS was significantly slower as the value of $t_{0.5}$ extracted was higher than the entire FRAP experiment (500 s), using an exponential fit with $r_{square}=0.97$.

siRNA knockdowns

Tet-inducible U2OS cell lines expressing CFP-β-actin-MS2 were transfected with Dcp2 small interfering RNA (catalog no. 1299003, Oligo ID, HSS136535, Invitrogen) or negative control (catalog no. 12935-400) using Lipofectamine 2000 following the manufacturer's instructions. The mRNA expression levels of Dcp2 were examined by semi-quantitative RT-PCR from total RNA using Tri Reagent (Sigma) 72 h after siRNA transfection using primers: forward, 5′-ATGGAGACC-AAACGGGTGGAGATT-3′ and reverse, 5′-GGAACTTGCAATGTCC-ATTACATGC-3′. Expression levels were normalized to actin mRNA levels using primers forward, 5′-GTGCATTCCCTGTACGCCTC-3′ and reverse, 5′-CCAGGAAGGAAGGCTGGAAG-3′.

For FRAP experiments, 48 h after siRNA transfection cells were co-transfected with YFP–MS2 and CFP–Dcp1a using the PolyJet transfection reagent. After 24 h, cells were taken for FRAP experiments or starved with

EBSS for 4 h before each FRAP experiment. Colocalization of the YFP–MS2 with the CFP–Dcp1a was verified by acquiring the first and last image of each experiment in the CFP channel.

Real-time PCR

Total RNA was extracted using the Direct-zol RNA miniprep kit (ZYMO Research). After reverse transcription using qScript cDNA Synthesis Kit (Quanta Bio sciences), cDNA was amplified using the following primer pairs. Dcp2, forward, 5′-ATGGAGACCAAACGGGTGGA-3′, and reverse, 5′-AACCAATGGGCAAGTTCAATCT-3′; CFP–actin, forward, 5′-GGATCACTCTCGGCATGGAC-3′ and reverse 5′-TGCACATACC-GGAGCCATTG-3′; β-globin–CFP, forward, 5′-GGCAAAGAATTCAT-GGTGAGC-3′ and reverse, CGCTGAACTTGTGGCCGTT; HPRT1, forward, 5′-CGTGATTAGTGATGATGAACCAG-3′ and reverse, 5′-CGAGCAAGACGTTCAGTCCT-3′; and GAPDH, forward, 5′-TCTTC-CAGGAGCGAGATCCCT-3′ and reverse, 5′-TGCAAATGAGCCCCA-GCCTTCT-3′.

Real-time PCR was performed using PerfeCTa® SYBR® Green FastMix®, ROX™ (Quanta Bio Sciences) on a CFX-96 system (Bio-Rad). Analysis was performed with the Bio-Rad CFX manager. Relative levels of mRNA expression were measured as the ratio of the comparative threshold cycle (CT) to internal controls (GAPDH and HPRT1) mRNA.

Acknowledgements

We thank and remember our beloved lab member, the late Noa Neufeld, who assisted with the FRAP experiments.

Competing interests

The authors declare no competing interests.

Author contributions

A.A. and Y.S.-T. conceived of and designed the experiments. A.A. performed the experiments, and was assisted by A.K. (FRAPs, Dcp2 KD, qFISH), P.K. (Dcp2 KD, qFISH), A.S. (image analysis), R.B.-Y. (CFP-Dcp1b cloning, live cell imaging), A.J. (image analysis) and N.K. (Dcp2 KD, western, qPCR, ActD). Y.S.-T. wrote the paper.

Funding

Y.S.-T. is supported by the European Research Council (ERC).

Supplementary material

Supplementary material available online at
http://jcs.biologists.org/lookup/suppl/doi:10.1242/jcs.152975/-/DC1

References

Aizer, A. and Shav-Tal, Y. (2008). Intracellular trafficking and dynamics of P bodies. *Prion* **2**, 131-134.
Aizer, A., Brody, Y., Ler, L. W., Sonenberg, N., Singer, R. H. and Shav-Tal, Y. (2008). The dynamics of mammalian P body transport, assembly, and disassembly in vivo. *Mol. Biol. Cell* **19**, 4154-4166.
Aizer, A., Kafri, P., Kalo, A. and Shav-Tal, Y. (2013). The P body protein Dcp1a is hyper-phosphorylated during mitosis. *PLoS ONE* **8**, e49783.
Andrei, M. A., Ingelfinger, D., Heintzmann, R., Achsel, T., Rivera-Pomar, R. and Lührmann, R. (2005). A role for eIF4E and eIF4E-transporter in targeting mRNPs to mammalian processing bodies. *RNA* **11**, 717-727.
Bail, S. and Kiledjian, M. (2006). More than 1 + 2 in mRNA decapping. *Nat. Struct. Mol. Biol.* **13**, 7-9.
Ben-Ari, Y., Brody, Y., Kinor, N., Mor, A., Tsukamoto, T., Spector, D. L., Singer, R. H. and Shav-Tal, Y. (2010). The life of an mRNA in space and time. *J. Cell Sci.* **123**, 1761-1774.
Bertrand, E., Chartrand, P., Schaefer, M., Shenoy, S. M., Singer, R. H. and Long, R. M. (1998). Localization of ASH1 mRNA particles in living yeast. *Mol. Cell* **2**, 437-445.
Bhattacharyya, S. N., Habermacher, R., Martine, U., Closs, E. I. and Filipowicz, W. (2006). Relief of microRNA-mediated translational repression in human cells subjected to stress. *Cell* **125**, 1111-1124.
Brengues, M. and Parker, R. (2007). Accumulation of polyadenylated mRNA, Pab1p, eIF4E, and eIF4G with P-bodies in Saccharomyces cerevisiae. *Mol. Biol. Cell* **18**, 2592-2602.
Brengues, M., Teixeira, D. and Parker, R. (2005). Movement of eukaryotic mRNAs between polysomes and cytoplasmic processing bodies. *Science* **310**, 486-489.
Brody, Y. and Shav-Tal, Y. (2011). Measuring the kinetics of mRNA transcription in single living cells. *J. Vis. Exp.* **54**, e2898.
Brody, Y., Neufeld, N., Bieberstein, N., Causse, S. Z., Böhnlein, E. M., Neugebauer, K. M., Darzacq, X. and Shav-Tal, Y. (2011). The in vivo kinetics of RNA polymerase II elongation during co-transcriptional splicing. *PLoS Biol.* **9**, e1000573.
Carbonaro, M., O'Brate, A. and Giannakakou, P. (2011). Microtubule disruption targets HIF-1alpha mRNA to cytoplasmic P-bodies for translational repression. *J. Cell Biol.* **192**, 83-99.
Cougot, N., Babajko, S. and Séraphin, B. (2004). Cytoplasmic foci are sites of mRNA decay in human cells. *J. Cell Biol.* **165**, 31-40.
Cougot, N., Cavalier, A., Thomas, D. and Gillet, R. (2012). The dual organization of P-bodies revealed by immunoelectron microscopy and electron tomography. *J. Mol. Biol.* **420**, 17-28.
Decker, C. J. and Parker, R. (2012). P-bodies and stress granules: possible roles in the control of translation and mRNA degradation. *Cold Spring Harb. Perspect. Biol.* **4**, a012286.
Eulalio, A., Behm-Ansmant, I. and Izaurralde, E. (2007a). P bodies: at the crossroads of post-transcriptional pathways. *Nat. Rev. Mol. Cell Biol.* **8**, 9-22.
Eulalio, A., Behm-Ansmant, I., Schweizer, D. and Izaurralde, E. (2007b). P-body formation is a consequence, not the cause, of RNA-mediated gene silencing. *Mol. Cell. Biol.* **27**, 3970-3981.
Fenger-Grøn, M., Fillman, C., Norrild, B. and Lykke-Andersen, J. (2005). Multiple processing body factors and the ARE binding protein TTP activate mRNA decapping. *Mol. Cell* **20**, 905-915.
Franks, T. M. and Lykke-Andersen, J. (2007). TTP and BRF proteins nucleate processing body formation to silence mRNAs with AU-rich elements. *Genes Dev.* **21**, 719-735.
Fusco, D., Accornero, N., Lavoie, B., Shenoy, S. M., Blanchard, J. M., Singer, R. H. and Bertrand, E. (2003). Single mRNA molecules demonstrate probabilistic movement in living mammalian cells. *Curr. Biol.* **13**, 161-167.
Gallina, M. E., Xu, J., Dertinger, T., Aizer, A., Shav-Tal, Y. and Weiss, S. (2013). Resolving the spatial relationship between intracellular components by dual color super resolution optical fluctuations imaging (SOFI). *Opt. Nanoscopy* **2**, 2.
Harding, H. P., Novoa, I., Zhang, Y., Zeng, H., Wek, R., Schapira, M. and Ron, D. (2000). Regulated translation initiation controls stress-induced gene expression in mammalian cells. *Mol. Cell* **6**, 1099-1108.
Hoyle, N. P., Castelli, L. M., Campbell, S. G., Holmes, L. E. and Ashe, M. P. (2007). Stress-dependent relocalization of translationally primed mRNPs to cytoplasmic granules that are kinetically and spatially distinct from P-bodies. *J. Cell Biol.* **179**, 65-74.
Ingelfinger, D., Arndt-Jovin, D. J., Lührmann, R. and Achsel, T. (2002). The human LSm1-7 proteins colocalize with the mRNA-degrading enzymes Dcp1/2 and Xrnl in distinct cytoplasmic foci. *RNA* **8**, 1489-1501.
Iwaki, A. and Izawa, S. (2012). Acidic stress induces the formation of P-bodies, but not stress granules, with mild attenuation of bulk translation in Saccharomyces cerevisiae. *Biochem. J.* **446**, 225-233.
Izaurralde, E. (2009). Freedom versus constraint in protein function. *Nat. Rev. Mol. Cell Biol.* **10**, 372.
Kedersha, N. and Anderson, P. (2009). Regulation of translation by stress granules and processing bodies. *Prog. Mol. Biol. Transl. Sci.* **90**, 155-185.
Kedersha, N., Stoecklin, G., Ayodele, M., Yacono, P., Lykke-Andersen, J., Fritzler, M. J., Scheuner, D., Kaufman, R. J., Golan, D. E. and Anderson, P. (2005). Stress granules and processing bodies are dynamically linked sites of mRNP remodeling. *J. Cell Biol.* **169**, 871-884.
Kimball, S. R. (2002). Regulation of global and specific mRNA translation by amino acids. *J. Nutr.* **132**, 883-886.
Kulkarni, M., Ozgur, S. and Stoecklin, G. (2010). On track with P-bodies. *Biochem. Soc. Trans.* **38**, 242-251.
Lavut, A. and Raveh, D. (2012). Sequestration of highly expressed mRNAs in cytoplasmic granules, P-bodies, and stress granules enhances cell viability. *PLoS Genet.* **8**, e1002527.
Liu, J., Valencia-Sanchez, M. A., Hannon, G. J. and Parker, R. (2005). MicroRNA-dependent localization of targeted mRNAs to mammalian P-bodies. *Nat. Cell Biol.* **7**, 719-723.
Lykke-Andersen, J. (2002). Identification of a human decapping complex associated with hUpf proteins in nonsense-mediated decay. *Mol. Cell. Biol.* **22**, 8114-8121.
Mollet, S., Cougot, N., Wilczynska, A., Dautry, F., Kress, M., Bertrand, E. and Weil, D. (2008). Translationally repressed mRNA transiently cycles through stress granules during stress. *Mol. Biol. Cell* **19**, 4469-4479.
Mor, A., Suliman, S., Ben-Yishay, R., Yunger, S., Brody, Y. and Shav-Tal, Y. (2010). Dynamics of single mRNP nucleocytoplasmic transport and export through the nuclear pore in living cells. *Nat. Cell Biol.* **12**, 543-552.
Ni, H. M., Bockus, A., Wozniak, A. L., Jones, K., Weinman, S., Yin, X. M. and Ding, W. X. (2011). Dissecting the dynamic turnover of GFP-LC3 in the autolysosome. *Autophagy* **7**, 188-204.
Parker, R. and Sheth, U. (2007). P bodies and the control of mRNA translation and degradation. *Mol. Cell* **25**, 635-646.
Parker, R. and Song, H. (2004). The enzymes and control of eukaryotic mRNA turnover. *Nat. Struct. Mol. Biol.* **11**, 121-127.
Pauley, K. M., Eystathioy, T., Jakymiw, A., Hamel, J. C., Fritzler, M. J. and Chan, E. K. (2006). Formation of GW bodies is a consequence of microRNA genesis. *EMBO Rep.* **7**, 904-910.
Pillai, R. S., Bhattacharyya, S. N., Artus, C. G., Zoller, T., Cougot, N., Basyuk, E., Bertrand, E. and Filipowicz, W. (2005). Inhibition of translational initiation by Let-7 MicroRNA in human cells. *Science* **309**, 1573-1576.

Sheth, U. and Parker, R. (2003). Decapping and decay of messenger RNA occur in cytoplasmic processing bodies. *Science* **300**, 805-808.
Simon, E., Camier, S. and Séraphin, B. (2006). New insights into the control of mRNA decapping. *Trends Biochem. Sci.* **31**, 241-243.
Stöhr, N., Lederer, M., Reinke, C., Meyer, S., Hatzfeld, M., Singer, R. H. and Hüttelmaier, S. (2006). ZBP1 regulates mRNA stability during cellular stress. *J. Cell Biol.* **175**, 527-534.
Sweet, T. J., Boyer, B., Hu, W., Baker, K. E. and Coller, J. (2007). Microtubule disruption stimulates P-body formation. *RNA* **13**, 493-502.
Takahashi, S., Sakurai, K., Ebihara, A., Kajiho, H., Saito, K., Kontani, K., Nishina, H. and Katada, T. (2011). RhoA activation participates in rearrangement of processing bodies and release of nucleated AU-rich mRNAs. *Nucleic Acids Res.* **39**, 3446-3457.
Teixeira, D., Sheth, U., Valencia-Sanchez, M. A., Brengues, M. and Parker, R. (2005). Processing bodies require RNA for assembly and contain nontranslating mRNAs. *RNA* **11**, 371-382.
van der Laan, A. M., van Gemert, A. M., Dirks, R. W., Noordermeer, J. N., Fradkin, L. G., Tanke, H. J. and Jost, C. R. (2012). mRNA cycles through hypoxia-induced stress granules in live Drosophila embryonic muscles. *Int. J. Dev. Biol.* **56**, 701-709.
van Dijk, E., Cougot, N., Meyer, S., Babajko, S., Wahle, E. and Séraphin, B. (2002). Human Dcp2: a catalytically active mRNA decapping enzyme located in specific cytoplasmic structures. *EMBO J.* **21**, 6915-6924.
Weil, T. T., Parton, R. M., Herpers, B., Soetaert, J., Veenendaal, T., Xanthakis, D., Dobbie, I. M., Halstead, J. M., Hayashi, R., Rabouille, C. et al. (2012). Drosophila patterning is established by differential association of mRNAs with P bodies. *Nat. Cell Biol.* **14**, 1305-1315.
Yang, Z., Jakymiw, A., Wood, M. R., Eystathioy, T., Rubin, R. L., Fritzler, M. J. and Chan, E. K. (2004). GW182 is critical for the stability of GW bodies expressed during the cell cycle and cell proliferation. *J. Cell Sci.* **117**, 5567-5578.
Yunger, S., Rosenfeld, L., Garini, Y. and Shav-Tal, Y. (2010). Single-allele analysis of transcription kinetics in living mammalian cells. *Nat. Methods* **7**, 631-633.
Yunger, S., Rosenfeld, L., Garini, Y. and Shav-Tal, Y. (2013). Quantifying the transcriptional output of single alleles in single living mammalian cells. *Nat. Protoc.* **8**, 393-408.
Zheng, D., Ezzeddine, N., Chen, C. Y., Zhu, W., He, X. and Shyu, A. B. (2008). Deadenylation is prerequisite for P-body formation and mRNA decay in mammalian cells. *J. Cell Biol.* **182**, 89-101.
Zurla, C., Lifland, A. W. and Santangelo, P. J. (2011). Characterizing mRNA interactions with RNA granules during translation initiation inhibition. *PLoS ONE* **6**, e19727.

Journal of Cell Science